ZANCO Journal of Pure and Applied Sciences
The official scientific journal of Salahaddin University-Erbil
https://zancojournals.su.edu.krd/index.php/JPAS

ISSN (print):2218-0230**, ISSN (online):** 2412-3986**, DOI: http://dx.doi.org/10.21271/zjpas**

RESEARCH PAPER

Production and Comparison of biochar derived from slow pyrolysis and ash from burnt of wheat straw residue

Lana Farhad Ibrahim[1]* and F. S. Tariq[1]

1College of Agricultural Engineering Sciences, Salahaddin University-Erbil, Kurdistan Reign, Iraq.

A B S T R A C T:

The pyrolysis of agricultural residues seems to be a new strategy to improve soil quality and keep the environment clean. This research focused on the compare between physico-chemical properties of the biochar derived from pyrolysis of wheat straw (WSB) at 500°C for a holding time of 2 h and the Ash was produced by burning wheat straw in an open field (WSA). Furthermore, the WSB and WSA were characterized for their chemical and physical properties. In addition, SEM, BET, FTIR were used to find morphological, surface area and functional groups of WSB and WSA. The results showed that WSB had more carbon content (63.76%) than WSA (9,174 %), which is indicated that biochar that more carbonized, hydrophobic and aromatic nature. Also, WSB had higher surface area and pore volume than WSA. However, WSA had more ash content, pH, EC values than WSB. Moreover, the SEM image exhibited that the surface area in the WSB was homogenous and arranged orderly while the WSA image presented that the surface area was crushed and untidy. The FTIR results obtained similar in functional groups for both samples. Biochar's high carbon, surface area and pore volume make it a promising tool to remediate polluted environments; it can also be used to enhance soil fertility through a liming effect, by adding volatile organic compounds and expanding the soil pore space.

KEY WORDS: Bread wheat,Wheat yield, Seeding rate, Previous crop, Different arable land
DOI: http://dx.doi.org/10.21271/ZJPAS.35.SpC.9
ZJPAS (2023) , 35(SpC);84-91 .

1. INTRODUCTION

Biochar, a carbon-rich material produced through the pyrolysis of biomass, has gained attention as a promising tool for mitigating climate change and promoting sustainable agriculture (Lehmann & Joseph, 2015). Biochar is known for its ability to sequester carbon, improve soil fertility, and reduce greenhouse gas emissions (Wang et al., 2016). In addition, it has the potential to be used in various applications such as water treatment, energy storage, and as a sustainable alternative to fossil fuels (Masek et al., 2017).

One of the most widely used feedstock for biochar production is agricultural waste, particularly wheat straw residue (Ahmad et al., 2014). Wheat straw is a cheap and abundant biomass resource that is produced in large quantities worldwide. According to the FAO (2022), approximately 8 million hectares of Iraqi land is utilized for agriculture. Alhassany et al. (2022) conducted a study which revealed that Iraq produces about 10 million tons of agricultural residues annually. The use of wheat straw as a feedstock for biochar production not only provides a sustainable solution to agricultural waste management but also offers a potential source of revenue for farmers (Yao et al., 2012).

Slow pyrolysis, a thermal process in which biomass is heated in the absence of oxygen, is a commonly used technique for biochar production from wheat straw (Ahmad et al., 2014). Slow pyrolysis offers several advantages over other pyrolysis techniques, including higher yields of biochar and lower energy requirements. Moreover, the process yields two valuable byproducts: bio-oil and syngas, which can be used as renewable energy sources.

Another potential application of wheat straw residue is the production of ash through controlled burning. Ash is a byproduct of the combustion

* **Corresponding Author:**
Lana Farhad Ibrahim1
E-mail: lanafarhad35@gmail.com
Article History:
Received: 07/02/2023
Accepted: 25/04 /2023
Published: 01/ 11/2023

process and consists of the inorganic mineral content of the biomass feedstock (Wang et al., 2016). Wheat straw ash has been shown to have potential as a fertilizer, particularly for crops with high potassium requirements (Lehmann & Joseph, 2015).

Characterization of biochar and ash from wheat straw residue is essential to assess their suitability for various applications. The properties of biochar, such as its surface area, porosity, and chemical composition, affect its performance in soil amendment and carbon sequestration. Similarly, the chemical composition and mineral content of wheat straw ash can affect its fertilization potential.

In recent years, several studies have focused on the production and characterization of biochar and ash derived from wheat straw residue. These studies have investigated various parameters such as pyrolysis temperature, heating rate, and residence time, to optimize biochar yield and properties (Ahmad et al., 2014). Additionally, the properties of wheat straw ash have been characterized to assess its potential as a fertilizer (Lehmann & Joseph, 2015).

The particular properties of the biomass material should be examined to better understand its pyrolysis behavior in order to investigate the possibilities of new biomass as a feedstock for biochar. According to our knowledge, there has not been comprehensive research on the biochar production from wheat straw and its characterization in the Kurdistan region and Iraq. This research clarifies the differences between biochar and ash derived from burned wheat straw. It will serve as a gateway for further investigation into wheat straw pyrolysis. Thus, this study focused on the impact of slow pyrolysis on the productivity and physicochemical characteristics of wheat straw biochar; then, it compared those characteristics with ash produced from burning wheat straw. This study assists in the future utilization biochar and ash for specific purposes with desirable properties.

2. Materials and methods

2.1 Collection of raw materials and preparation of Biochar and Ash

About 100 kg of chopped wheat straw were collected from Erbil Feed Factory in Erbil, Kurdistan Region-Iraq. and then washed with distilled water to avoid any dust or dirt before oven drying at 105 ◦C for 12 h according to the method reported by (Li et al., 2020 a,b). The dried chopped wheat straws were exposed to slow pyrolysis in large chamber muffle furnace that digitally regulated temperature which is about 11 L volume (38 cm (length) × 17 cm (width) × 17 cm (height), (Make: Nitin Scientific Industries, New Delhi - 220/230V AC supply, PID Controlled) for two hours at a predetermined temperature 500 Cº. In addition, wheat ash was produced by burning chopped wheat straw in an open air with presence of oxygen. After that, samples cooled at room temperature. Triplicate samples were prepared for both biochar and ash, and their mean values were reported. Subsequently, both the biochar and ash were finely processed and passed through a 1-mm sieve before being stored at room temperature for analysis. The samples were analyzed to distinguish between the chemical and physical properties of the biochar and ash.

2.2 Characterization of Biochar and Ash

The pH and EC of the ash and biochar samples were determined by mixing 1 g of sample with 100 and 20 mL distilled water respectively (Samsuri et al., 2021). Dry combustion method was applied to measure ash content, in brief about 5.0 g of biochar was heated to 500 °C for 8 hours in large chamber muffle furnace (Make: Nitin Scientific Industries, New Delhi - 220/230V AC supply, PID Controlled). After that waiting for the crucible to return to ambient temperature, it was reweighed. The percentage of ash content was then calculated based on weight loss.

The cation exchange capacity (CEC) is determined using the procedure reported by (Sond and Guos, 2012). Nitrogen, C, S and C/N ratio were determined by using elemental analyzer (model: LECO TruMac CNS Analyzer) according to the procedure reported by (Tariq et al., 2016). The total element content in the Ash and Biochar samples were measured by ICP-OES after digesting approximately 0.25 g of sample with of 2 mL of 30% H_2O_2 and 6 mL of 65% HNO_3 in microwave digestion system; according to the digestion program explained by (Traiq. et al., 2016). The FTIR (Fourier Transformed Infrared Spectroscopy) (Perkin Elmer AFTIR-2000 spectrometer) was utilized for identifying the active organic functional groups of samples. The Brunauer–Emmett–Teller (BET) approach (TriStar II Plus Serial # 283 Unit 1 Port 1 Version 2.0) was used to determine the surface area of the Biochar and Ash samples. The WSB and WSA morphology was measured by using The Scanning

Electron Microscope-Electron Dispersive Spectroscopy (SEM-EDS).

3. Result and discussion

3.1 Chemical properties of WSB and WSA

Table (1) summarizes the chemical analysis data for the samples. The results indicated that the pH, EC, CEC and oxygen content of WSA was higher than WSB. The pH values for Biochar and Ash were 10.6 and 9.4 respectively. Tsai et al., (2012) explained that minerals included in the WSB and WSA begin separating from the organic matrix, which causes the pH to increase as the pyrolysis temperature increases. A separation of organic (carbon) and inorganic (ash) components has also been observed. Both of these pathways are responsible for the pH rise. These finding are relevance with Ahmad et al., (2012) and Al-Wabel et al., (2013). In addition, when their temperatures were elevated, WSA and WSB both showed an increase in their electrical conductivity (EC). WSB had an EC of 100 mS cm^{-1} whereas WSA's EC was 241 mS cm^{-1}. This difference could be contributed to the loss of volatile substances, which causes components to concentrate in the ash fraction (Cantrell et al., 2012). As a consequence of its extremely large surface area, negative surface charge, carbonate discharge, oxygenated functional groups on its surface, and oxide adsorption, it is assumed that biochar has a high cation exchange capacity (Hailegraw et al., 2019).

Table 1 also presents the elemental content of WSA and WSB that were tested. The result showed that carbon content for WSB was 63.76%.This findin similar to Domingues et al., (2017) who found that stronger polymerization caused the rise in carbon content in WSB, which in turn caused a more compacted carbon structure in biochar. The C content changed proportionally with the H and O losses. Hunt et al. (2010) studied the effect of temperature rate paralyzing on feedstock and found that about 50% of H ion is removed at 500 ^{0}C.

In addition, amounts of inorganic compounds observed in Biochar and ash samples such as Chlorine, silica, aluminum, and potassium were found, while their quantities varied substantially across samples. Si (17.38%) is the most abundant element in WSB, followed by K (10.20%), N (0.802) and P (0.151). However, in WSA O was predominated (90.268%), followed by K (16.15), Si (13.26), N (0.257) and P (0.74). As shown in Table 1 K values were lower in WSB owing to the low ash concentration compared to WSA, which contains a considerable quantity of K due to the ash level of over 50% (Table 1). However, the high nitrogen content in WSB may be due to the presence of resistant nitrogen in aromatic compounds (Kazi et al., 2011). In addition, the high P content of WSB results from the breaking of organic P bonds and the sublimation of carbon during pyrolysis (Gul et al., 2015).

Table 1. Chemical properties of WSB and WSA samples.

Parameter	WSB	WSA
pH	9.4	10.6
EC (mS cm^{-1})	100	241
CEC (cmolc kg-1)	1621	1300
O (%)	34.84	90.268
C (%)	63.76	9.174
H (%)	0.595	0.301
Ash content %	24.8	86.96
Si (%)	17.38	13.26
Cl (%)	6.69	4.33
K (%)	10.20	16.15
Al (%)	0.26	
Mg (%)	0.1	0.55
Na (%)	0.040	0.38
P (%)	0.151	0.74
S (%)	0.437	1.407
N (%)	0.802	0.257

3.2. Physical properties of WSB and WSA

The BET surface areas of WSB was 73.83 m^2 g^{-1} which was higher than WSA 0.980 m^2 g^{-1}. The higher value of BET for WSB may be related to the intense reactions at 500C° which leaves beh ind a larger micro pore structure, compared to WS A. Furthermore, higher surface area of WSB migh t be contributed to the release of more volatile co mpounds at higher temperatures during pyrolysis (Ahmad et al., 2012). Also, Arenas and Chejne (20 04) found that increasing the temperature results i n the formation of a porous structure in biochar an d the degradation of the pore walls. The total pore volume of biochar was 0.012 cm^3 g^{-1} and for ash was 0.001 cm^3 g^{-1} (Table 2), this variation in pore volume may be related to the shape of their cells (Lu & Zong, 2018). In Figure (1 and 2) clearly sho wed the structures of the biochar become more ordered and the pores become wider at treatment temperatures above 500°C (Angin et al., 2013). Morphology of biochar and Ash was determined through SEM images. In the SEM images (Figure 1 and 2) the micro holes, macrospores, and meso pores of the Biochar displayed a diversity of morphologies at 500°C, the biochar's shape became honeycomb-like with cylindrical holes and several huge linked holes. The micrographs of biochar reveal many pores produced uniformly over the surface and grouped in an ordered pattern. On the surface of the WSB biochar, a systematic arrangement of little perpendicular blocks may be seen. Therefore, the WSA's surface is more heterogeneous and powdered.

Table 2. Physical properties of wheat straw biochr and wheat straw ash

Parameter	WSB	WSA
BET surface area (m²/g)	73.83	0.980
Pore volume (cm³/g)	0.012	0.001
Pore size (nm)	6.640	44.08
Ash content %	24.80	86.96

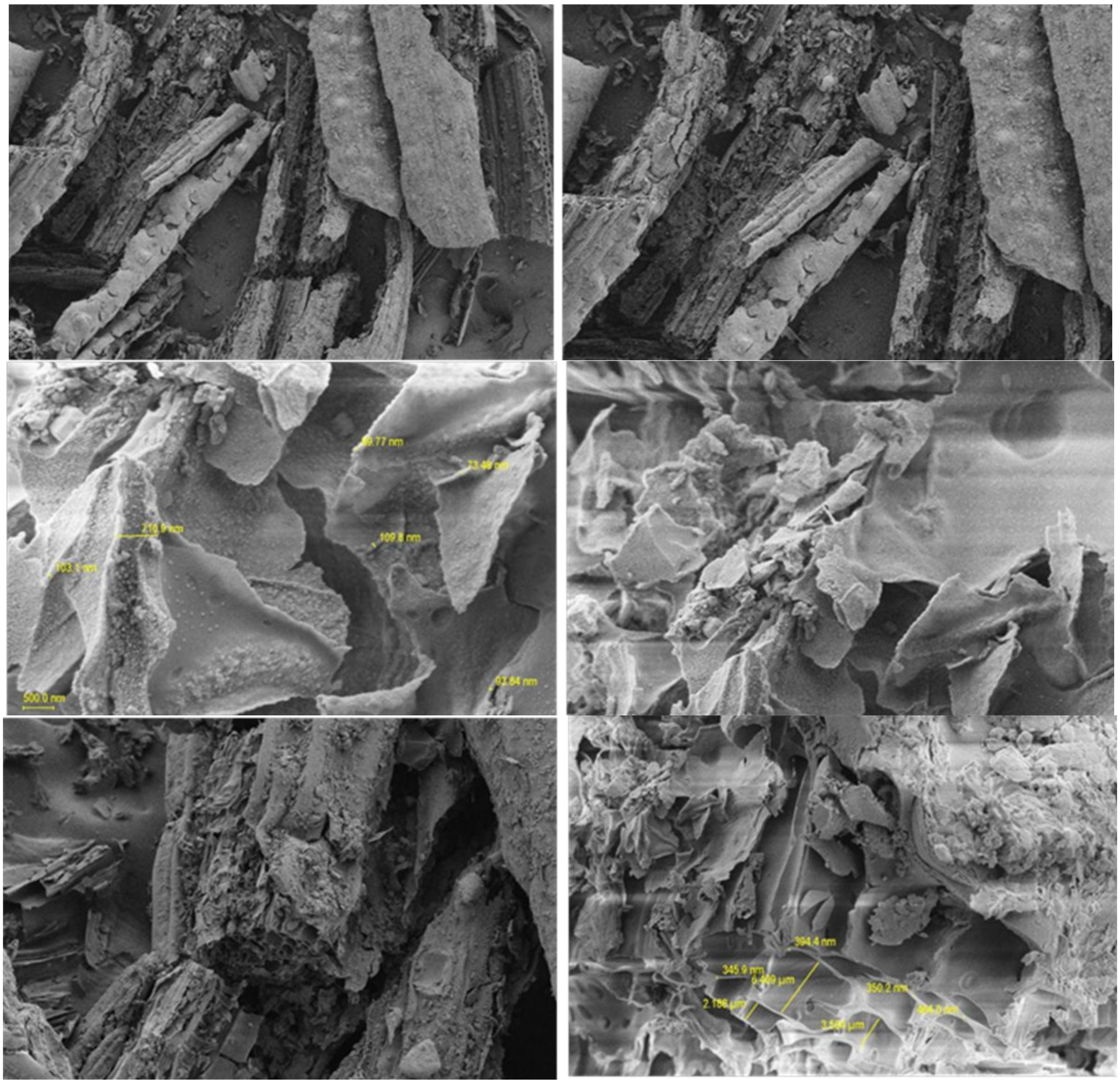

Figure 1. SEM images of wheat straw biochar produced at (500C°).

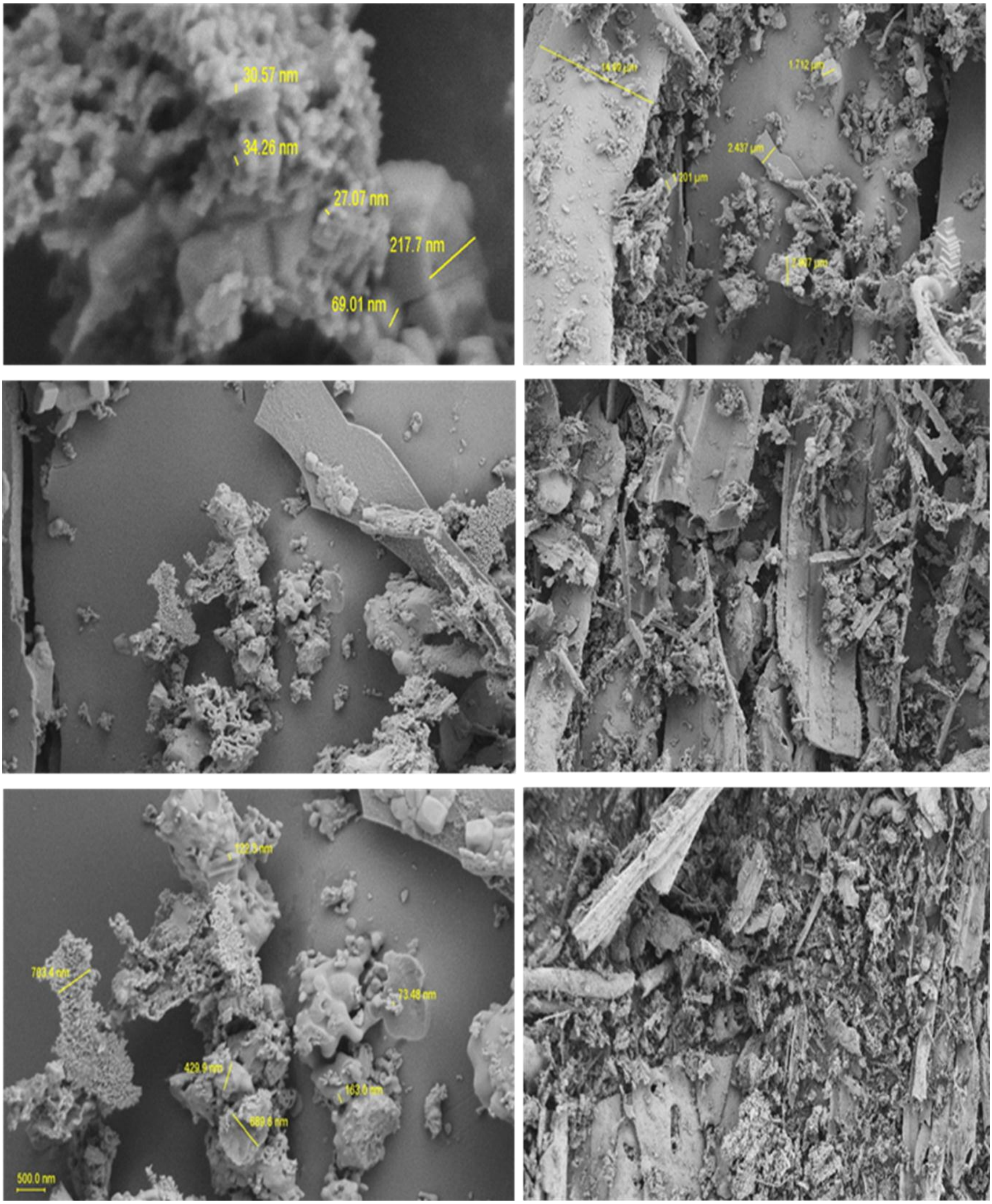

Figure 2. SEM images of wheat straw ash produced in open air with presence of oxygen

3.3. functional groups and structural modifications in WSB and WSA by Fourier-transform infrared spectroscopy (FTIR)

The FTIR spectroscopy is the best technique for identifying functional groups and structural modifications in materials (Jia et al.,2018). Figure (3) displays the FTIR spectra for WSB and WSA. In order to examine and convert the FTIR spectrums of WSB and WSA to their respective functional groups, the results of FTIR analysis were compared to earlier results obtained by Cao and Harris (2010), Chia et al. (2012), and (Xu et al. (2013). The first wide band peak in both WSB and WSA was (3640, 3465 cm^{-1}) wave number, and this values associated with the dehydration of biomass induced by phenols, alcohols, and carboxylic acids. It is mostly contributed to the stretching of the OH group (Camargo and Sene et al., 2014; Gupta et al., 2018). The asymmetric C–H stretching bands (2,924 cm^{-1}) were related to aliphatic functional groups. The secondary N–H bend (1550 to 1650 cm^{-1}) is present in both ash and biochar. Furthermore, The C=O stretching for carboxyl, aldehyde, ketone and ester were identified in the band width 1732 cm^{-1} (Caldero´n et al., 2006; Das et al., 2009). Hence, based on the FTIR spectra of WSB and WSA, the existence of aromatic C=C stretching and C=O stretching of chained compounds and ketones, O–H bending of phenols (1375 cm^{-1}), may be related to their FTIR spectral characteristics (Cantrell et al., 2012). The bands at 1300–1000 cm^{-1} are attributed to the stretching vibration of C–O, which is often seen in phenols or hydroxyl groups. Nevertheless, researchers expect that this band corresponds to the vibration of the C–O–C pyran ring skeleton (Jia et al.,2018). Furthermore, inorganic components such as sulfates and silicates can also contribute to the broad and intensive peak at 970–1200 cm^{-1} (Wen et al., 2007). The pinnacle of this region at band 1119 and1028 cm^{-1} was attributed to the symmetric C–O stretching for cellulose, hemicellulose, and lignin, which could be found in bedding material and partially digested feed (Caldero´n et al., 2006; Keiluweit et al., 2010). Both samples' FTIR spectra showed a reduction in H-bonded hydroxyl groups, which was ascribed to the pyrolysis temperature rising and increasing the dehydration process in the biomass (Chen et al., 2012).

B

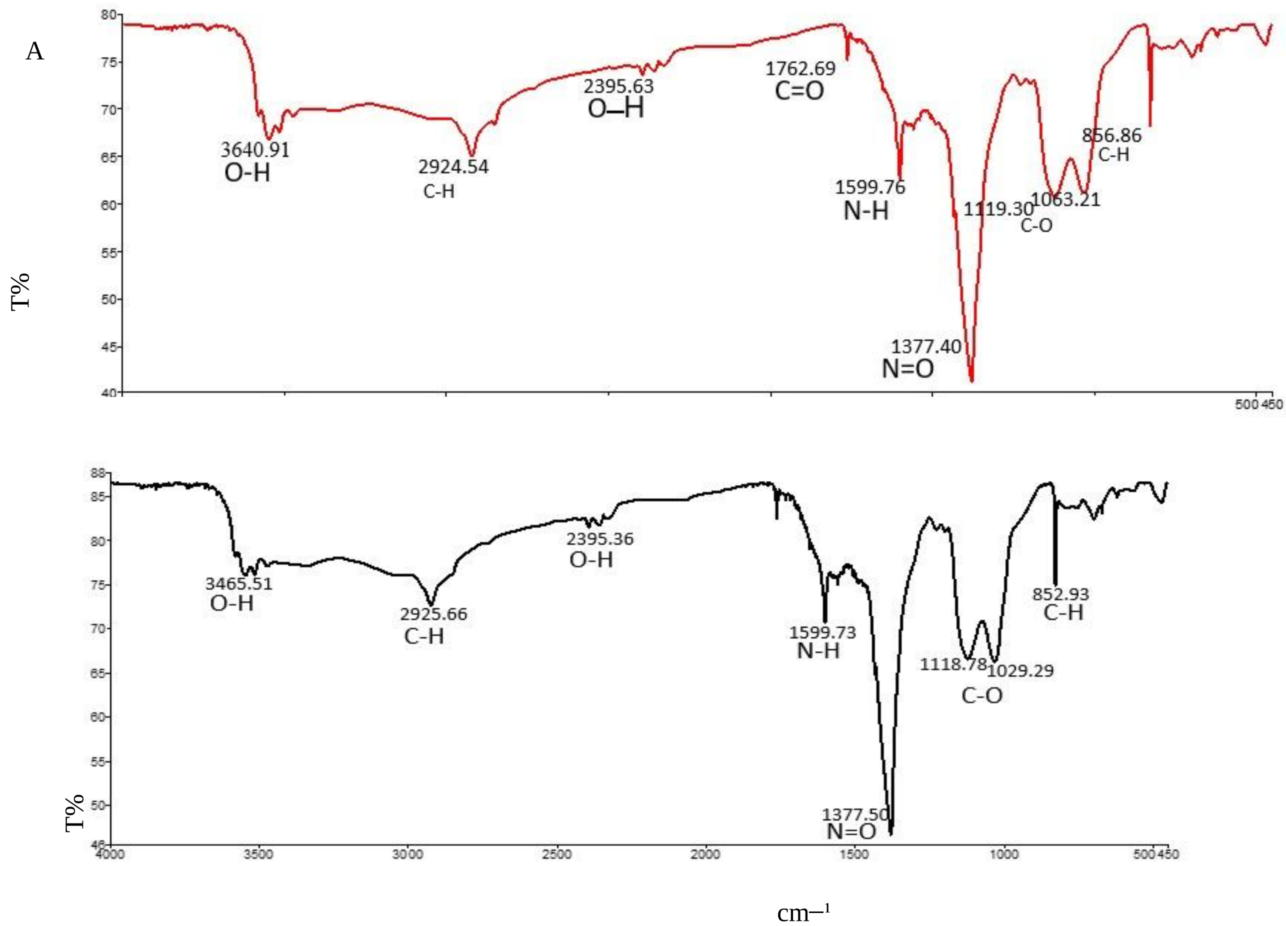

Figure 3. FTIR spectra peaks of WSB (A) and WSA (B)

4.Conclusion

Biochar derived from wheat straw and produced by slow pyrolysis at 500°C and Ash obtained from wheat straw and produced by open-air burning showed varied physical and chemical characteristics. Biochar's morphology and structure exhibit unique shape and form. The biochar generated pores on the surface in an ordered, varied size that formed homogenously and was suitable for soil application due to high CEC and high nutrient content . The ash had limited surface areas or inadequate formation of big pores, resulting in a more heterogeneous and crushed surface. While biochar became predominantly carbonaceous, dominating inorganic components considerably differed between the two samples. The pH of biochar was 9.4 this information may be utilized to develop optimal biomass usage pathways for energy or biochar synthesis. it is indicated that biochar from wheat straw is excellent for carbon sequestration and improving soil characteristics.

Rreffrences

Ahmad, M., Rajapaksha, A.U., Lim, J.E., Zhang, M., Bolan, N., Mohan, D., Vithanage, M., Lee, S.S., Ok, Y.S., 2014. Biochar as a sorbent for contaminant management in soil and water: a review. Chemosphere 99, 19–33. https://doi.org/10.1016/j.chemosphere.2013.10.071

.Ahmad, M., Lee, S.S., Dou, X., Mohan, D., Sung, J.K., Yang, J.E. and Ok, Y.S., 2012. Effects of pyrolysis temperature on soybean stover-and peanut shell-derived biochar properties and TCE adsorption in water. *Bioresource technology*, *118*, pp.536-544.

Alhassany, H.D., Abbas, S.M., Tostado-Véliz, M., Vera, D., Kamel, S. and Jurado, F., 2022. Review of Bioenergy Potential from the Agriculture Sector in Iraq. *Energies*, *15*(7), p.2678.

Al-Wabel, M.I., Al-Omran, A., El-Naggar, A.H., Nadeem, M. and Usman, A.R., 2013. Pyrolysis temperature induced changes in characteristics and chemical composition of biochar produced from conocarpus wastes. *Bioresource technology*, *131*, pp.374-379.

Angın, D., 2013. Effect of pyrolysis temperature and heating rate on biochar obtained from pyrolysis of safflower seed press cake. *Bioresource technology*, *128*, pp.593-597.

Arenas, E. and Chejne, F., 2004. The effect of the activating agent and temperature on the porosity development of physically activated coal chars. *Carbon*, *42*(12-13), pp.2451-2455.

Calderón, F.J., McCarty, G.W. and Reeves III, J.B., 2006. Pyrolisis-MS and FT-IR analysis of fresh and decomposed dairy manure. *Journal of Analytical and Applied Pyrolysis*, *76*(1-2), pp.14-23.

Cantrell, K.B., Hunt, P.G., Uchimiya, M., Novak, J.M. and Ro, K.S., 2012. Impact of pyrolysis temperature and manure source on physicochemical characteristics of biochar. *Bioresource technology*, *107*, pp.419-428.

Chen, Y., Yang, H., Wang, X., Zhang, S. and Chen, H., 2012. Biomass-based pyrolytic polygeneration system on cotton stalk pyrolysis: influence of temperature. *Bioresource technology*, *107*, pp.411-418.

Chia, C.H., Gong, B., Joseph, S.D., Marjo, C.E., Munroe, P. and Rich, A.M., 2012. Imaging of mineral-enriched biochar by FTIR, Raman and SEM–EDX. *Vibrational Spectroscopy*, *62*, pp.248-257.

Cao,X., Harris, W., 2010. Properties of dairy–manure–derived biochar pertinent to its potential use in remediation. Bioresour Technol 101: 5222–5228

Das, D.D., Schnitzer, M.I., Monreal, C.M. and Mayer, P., 2009. Chemical composition of acid–base fractions separated from biooil derived by fast pyrolysis of chicken manure. *Bioresource technology*, *100*(24), pp.6524-6532.

Domingues, R.R., Trugilho, P.F., Silva, C.A., Melo, I.C.N.D., Melo, L.C., Magriotis, Z.M. and Sanchez-Monedero, M.A., 2017. Properties of biochar derived from wood and high-nutrient biomasses with the aim of agronomic and environmental benefits. *PloS one*, *12*(5), p.e0176884.

FAO, 2022. Agricultural Value Chain Study in Iraq—Dates, Grapes, Tomatoes and Wheat. Baghdad, Iraq.

Gul, S., Whalen, J.K., Thomas, B.W., Sachdeva, V. and Deng, H., 2015. Physico-chemical properties and microbial responses in biochar-amended soils: mechanisms and future directions. *Agriculture, Ecosystems & Environment*, *206*, pp.46-59.

Hailegnaw, N.S., Mercl, F., Pračke, K., Száková, J. and Tlustoš, P., 2019. Mutual relationships of biochar and soil pH, CEC, and exchangeable base cations in a model laboratory experiment. *Journal of Soils and Sediments*, *19*, pp.2405-2416.

Hunt, J., DuPonte, M., Sato, D., Kawabata, A., 2010. The base of biochar: a natural soil amendment. Soil Crop Manag, 30, 1-4.

Jia, Y., Shi, S., Liu, J., Su, S., Liang, Q., Zeng, X. and Li, T., 2018. Study of the effect of pyrolysis temperature on the Cd2+ adsorption characteristics of biochar. *Applied Sciences*, *8*(7), p.1019.

Kazi, Z.H., Schnitzer, M.I., Monreal, C.M. and Mayer, P., 2010. Separation and identification of heterocyclic nitrogen compounds in biooil derived by fast pyrolysis of chicken manure. *Journal of Environmental Science and Health Part B*, *46*(1), pp.51-61.

Keiluweit, M., Nico, P.S., Johnson, M.G. and Kleber, M., 2010. Dynamic molecular structure of plant biomass-derived black carbon (biochar). *Environmental science & technology*, *44*(4), pp.1247-1253.

Li, W., Wang, D., Zhu, Y., Chen, J., Lu, Y., Li, S., Zheng, Y. and Zheng, Z., 2020a. Efficient ex-situ catalytic upgrading of biomass pyrolysis vapors to produce methylfurans and phenol over bio-based activated carbon. *Biomass and Bioenergy*, *142*, p.105794.

Li, Y., Xing, B., Ding, Y., Han, X. and Wang, S., 2020b. A critical review of the production and advanced utilization of biochar via selective pyrolysis of lignocellulosic biomass. *Bioresource Technology*, *312*, p.123614.

Lu, S. and Zong, Y., 2018. Pore structure and environmental serves of biochars derived from different feedstocks and pyrolysis conditions. *Environmental Science and Pollution Research*, *25*, pp.30401-30409.

Lehmann, J., Joseph, S., 2015. Biochar for environmental management: science, technology and implementation. Biochar for Environmental Management: Science and Technology https://doi.org/10.4324/9780203762264

Masek, J., Lubasova, D., Lukac, R., Turanek-Knotigova, P., Kulich, P., Plockova, J., et al. (2017). Multi-layered nanofibrous mucoadhesive films for buccal and sublingual administration of drug-delivery and vaccination nanoparticles - important step towards effective mucosal vaccines. J. Control Release 249, 183–195. doi: 10.1016/j.jconrel.2016.07.036

Samsuri, A.W., Tariq, F.S., Karam, D.S., Aris, A.Z. and Jamilu, G., 2019. The effects of rice husk ashes and inorganic fertilizers application rates on the phytoremediation of gold mine tailings by vetiver grass. *Applied Geochemistry*, *108*, p.104366.

Song, W. and Guo, M., 2012. Quality variations of poultry litter biochar generated at different pyrolysis temperatures. *Journal of analytical and applied pyrolysis*, *94*, pp.138-145.

Tsai, W.T., Liu, S.C., Chen, H.R., Chang, Y.M. and Tsai, Y.L., 2012. Textural and chemical properties of swine-manure-derived biochar pertinent to its potential use as a soil amendment. *Chemosphere*, *89*(2), pp.198-203.

Wang, D., Jiang, P., Zhang, H. and Yuan, W., 2020. Biochar production and applications in agro and forestry systems: A review. *Science of the Total Environment*, *723*, p.137775.

Wang, Q., II, R., Cai, H., Awasthi, M.K. Zhang, Z. Wang, J. Ali, A. Amanullah, M. 2016. Improving pig manure composting efficiency employing Ca-bentonite Ecol. Eng. 87, 157-161.

Wen, B., Zhang, J.J., Zhang, S.Z., Shan, X.Q., Khan, S.U. and Xing, B., 2007. Phenanthrene sorption to soil humic acid and different humin fractions. *Environmental Science & Technology*, *41*(9), pp.3165-3171.

Xu, X., Cao, X. and Zhao, L., 2013. Comparison of rice husk-and dairy manure-derived biochars for simultaneously removing heavy metals from aqueous solutions: role of mineral components in biochars. *Chemosphere*, *92*(8), pp.955-961.

Yao, Y.N.; Gao, B.; Chen, H.; Jiang, L.; Inyang, M.; Zimmerman, A.R. Adsorption of sulfamethoxazole on biochar and its impact on reclaimed water irrigation. J. Hazard. Mater. 2012, 209, 408–413.